

Compositionally Graded Microstructure for Ag-Fe Nanoparticles

Chandan Srivastava*, K. V. L. Sushma

(Received 11 July 2012; accepted 3 September 2012; published online 25 September 2012.)

Abstract: Ag-Fe nanoparticles with a highly Ag rich average composition were synthesized by the sonochemical route. Silver-iron system exhibits a wide miscibility gap in the bulk materials. Interestingly, a graded compositional profile along the nanoparticle radius was observed. Regions at and near the surface of the nanoparticle contained both Ag and Fe atoms. The composition got relatively deficient Fe towards the center of the particle with particle core made up of pure Ag. Alloying of Ag and Fe is confirmed by the absence of diffraction signal corresponding to pure Fe phase and presence of a paramagnetic phase in nanoparticles containing a diamagnetic (Ag) and ferromagnetic (Fe) elements.

Keywords: Nanoparticles; Electron Microscopy; Ag-Fe; Miscibility gap; Solid solution; Microstructure

Citation: Chandan Srivastava and K. V. L. Sushma, "Compositionally Graded Microstructure for Ag-Fe Nanoparticles", *Nano-Micro Lett.* 4 (3), 172-175 (2012). <http://dx.doi.org/10.3786/nml.v4i3.p172-175>

Introduction

Scientific and technological research endeavors in nanoscience and nanotechnology have gained significant momentum in the recent years. The growing interest is primarily due to two important incentives; (a) tunable functional properties and (b) realization of microstructures that cannot be obtained in the bulk systems with similar compositions and under similar conditions. With respect to the novel microstructures, one significant observation has been the formation of solid solution between atoms with a large difference in sizes (>14%) and a high positive enthalpy of mixing [1,2]. Such component atoms do not form a single phase solid solution in bulk for certain or overall composition ranges. This phenomenon is known as miscibility gap [3]. Nano-size induced miscibility has been reported for several bulk immiscible binary systems such as Ag-Pt [4], Ag-Ni [5], Ag-Co [6], Au-Pt [7], Pt-Ru [8] etc.

For isolated nanoparticles, the extent of miscibility and thus the resultant particle microstructure is primarily controlled by the particle size and particle composition. For spherical nanoparticles, particle size

provides thermodynamic stability to the solid solution phase due to the energetic contribution from the curvature [9,10]. Increase in the curvature enhances solid solubility in accordance with the Gibbs Thompson effect [9,10]. Compositional dependence stems from the fact that energetic contribution from the positive enthalpy of mixing increases with composition achieving maximum value for the equi-atomic composition [11]. Therefore, a nano-sized particle in which one of the component element atoms is present in a relatively lower amount as solute can possibly retain a thermodynamically stable single phase solid solution microstructure from the synergetic effect of nano size and lower positive enthalpy of mixing value.

The present work investigates the nanoparticle microstructure for Ag-Fe nanoparticles containing very low concentration of Fe as solute. The nanoparticles were synthesized by the sonochemical route [12]. It should be noted that the silver-iron system in bulk exhibits a wide miscibility gap extending into the liquid region [13]. The wide immiscibility between Ag and Fe is primarily due to the large atomic size difference (~14%) and a positive enthalpy of mixing value of 28

Department of Materials Engineering, Indian Institute of Science, Bangalore, India

*Corresponding author. E-mail: csrivastava@materials.iisc.ernet.in

kJ/mol [13].

Experiment

To synthesize the Ag-Fe nanoparticles, silver nitrate (AgNO_3) and ferric nitrate ($\text{Fe}(\text{NO}_3)_3 \cdot 9\text{H}_2\text{O}$) were used as precursors for Ag and Fe respectively. Calculated quantities of the precursors together with Polyvinylpyrrolidone (PVP) surfactant were transferred into a three neck round bottom flask containing de-ionized water acting as solvent. Synthesis reaction was carried out in an inert (argon) atmosphere. The round bottom flask containing the reaction mixture was placed in a bath sonicator. The reaction mixture was sonicated for about 10 minutes to facilitate uniform mixing of the precursors and flushing out of the oxygen from the flask. After 10 minutes, a reducing agent that was alkyl solution of sodium borohydride was added dropwise into the reaction mixture. After the addition of the reducing agent, sonication was continued for about another one hour. After one hour the reaction mixture was allowed to cool down to the room temperature under the argon atmosphere, following which the reaction mixture was dropped into a flask containing 100ml of ethanol. The nanoparticles settled at the bottom of the flask were then separated by centrifuging and repeatedly washed in ethanol.

Average composition of the nanoparticle dispersion was determined by the energy dispersive spectroscopy (EDS) technique using a Quanta ESEM scanning electron microscope (SEM) operating at 20 kV. A 300 keV field emission FEI Tecnai F-30 transmission electron microscope (TEM) was used for obtaining bright field images, selected area electron diffraction patterns, and compositional information from as-synthesized nanoparticles. Sample for the TEM based analysis was prepared by drop drying a highly dilute dispersion of the as-synthesized nanoparticles on an electron transparent carbon coated Cu grid. The magnetic hysteresis loop for the as-synthesized nanoparticles was obtained using a Lakeshore Vibrating Sample Magnetometer (VSM).

Result and discussion

Average composition for the as-synthesized nanoparticle dispersion obtained from the SEM-EDS analysis was 97 wt% Ag. A representative SEM-EDS profile obtained from the as-synthesized nanoparticles is shown in Fig. 1. Bright field TEM image of the as-synthesized nanoparticles is shown in Fig. 2. It can be seen from the Fig. 2 that the as-synthesized nanoparticles are nearly spherical shaped. Average particle size and standard deviation of particle size distribution obtained from the analysis of about 300 particles was 16 nm and 3 nm

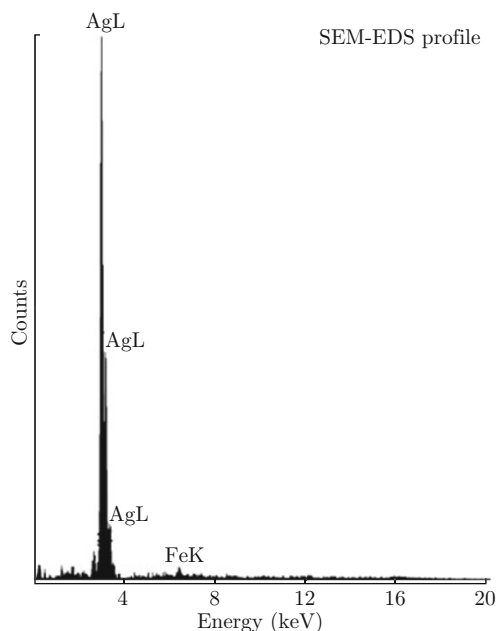


Fig. 1 Representative SEM-EDS curve for as-synthesized nanoparticles.

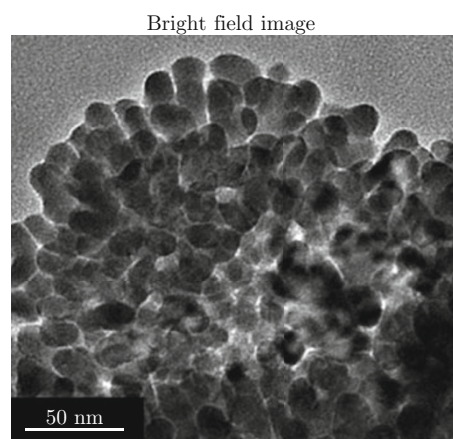


Fig. 2 TEM bright field image of as-synthesized nanoparticles.

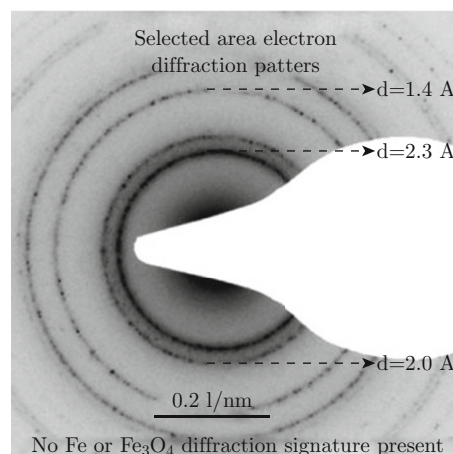


Fig. 3 Selected area electron diffraction pattern from as-synthesized nanoparticles.

respectively. Figure 3 shows selected area electron diffraction (SAED) pattern obtained from a large group of nanoparticles. The selected area electron diffraction pattern does not show any peak corresponding to the pure iron or magnetite phase. The absence of pure iron or magnetite phase diffraction signals indicate the non-detectable amounts of pure Fe or Fe_3O_4 phase in the as-synthesized nanoparticle dispersion. The d-spacing corresponding to the different planar spacings in the crystal of the pure Fe and Fe_3O_4 can be found in the JCPDS file numbers 85-1410 and 86-1362, respectively.

Scanning transmission electron microscopy (STEM) image of the as-synthesized nanoparticles is shown in Fig. 4(a). STEM-EDS compositional profile obtained along the diameter of an individual nanoparticle is shown in Fig. 4(b). In the STEM-EDS experiment, compositional information was obtained by analyzing the X-rays emitted from scanning a nano-sized electron probe (~ 1 nm in diameter) along the line denoted by AB in the Fig. 4(a). It can be seen from the compositional profile in Fig. 4(b) that the regions near the particle surface contain both Ag and Fe atoms. Near surface regions are relatively richer in Fe as compared to the inside of particle and the amount of Fe gradually decreases towards the center of the particle. The center of the particle is composed of almost pure Ag.

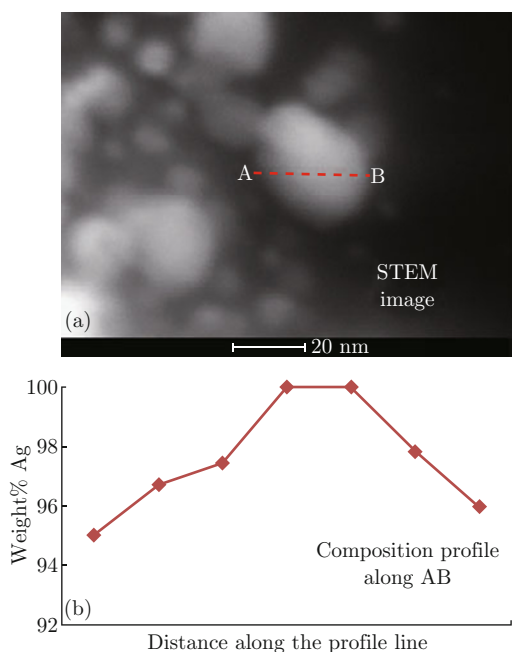


Fig. 4 (a) STEM image of nanoparticles, (b) compositional line profile plot obtained from the compositional analysis along the line AB in figure 4(a).

Field dependent initial magnetization curve (principle curve) for the as-synthesized nanoparticles measured at the room temperature using a 2 tesla field is shown in Fig. 5(a). The whole magnetic hysteresis loop showing the presence of magnetic coercivity (~ 30

Oe) in the as-synthesized sample is shown in Fig. 5(b). The initial magnetization curve reveals a rapid increase in the magnetization followed by a linearly increasing trend with a constant slope for the higher field values. Profile of the magnetization curve and the presence of magnetic coercivity thus clearly indicate the presence of two different magnetic phases. They are ferromagnetic and paramagnetic phases. Ferromagnetic component has been separated from the initial magnetization curve by subtracting the paramagnetic component from the total magnetization in the high field regions. The ferromagnetic and the paramagnetic curves are separately indicated in Fig. 5(a).

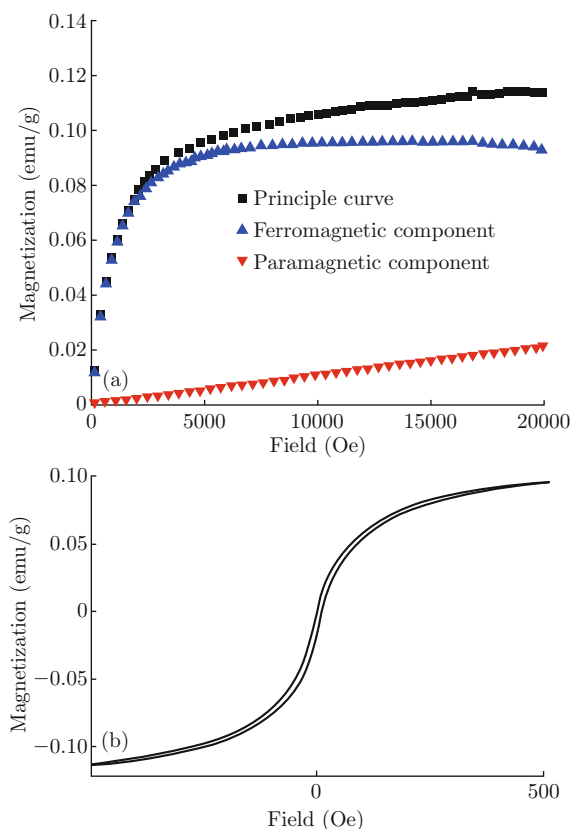


Fig. 5 (a) Field dependent initial magnetization curve (principle curve) for the as-synthesized nanoparticles measured at the room temperature using a 2 tesla field, (b) magnetic hysteresis loop obtained from the nanoparticles showing the presence of magnetic coercivity.

Absence of diffraction signatures corresponding to the ferromagnetic pure Fe and Fe_3O_4 phases in the electron diffraction pattern and a compositionally graded profile along the nanoparticle radius indicates that the two different magnetic behaviors denoted by the initial magnetization curve most certainly correspond to the presence of a ferromagnetic and a paramagnetic phase within a particle. It should be noted that pure Ag is diamagnetic and pure Fe is ferromagnetic. The overall high Ag rich average composition along with an ab-

sence of a diamagnetic signal and presence of a paramagnetic phase strongly indicates alloying of Ag and Fe atoms co-present at and near the surface of the particle. Paramagnetic character for highly dilute solid solutions phase formed between a diamagnetic and ferromagnetic element where the ferromagnetic atom forms the solute has been well observed for bulk miscible systems such as Ni-Cu and Cu-Fe [14]. Paramagnetic character has also been reported for Ag-rich, solid solution Ag-Ni system which is similar to the Ag-Fe system both with respect to the magnetic nature of the component element atoms and with respect to the immiscibility in the bulk state [15]. The ferromagnetic component with an extremely low value of the saturation magnetization (~ 0.001 emu/g) and coercivity (~ 30 Oe) can be due to the presence of very small amount of ferromagnetic Ag-oxide impurity on the surface of the Ag-Fe nanoparticles. It has been shown by Jo et al. [16] that ~ 7 nm sized Ag-Cu nanoparticles with an Ag-core and Cu-oxide shell microstructure contain a paramagnetic and a ferromagnetic phase. The Cu-oxide forms the paramagnetic phase and the ferromagnetism with a saturation magnetization and the coercivity values of 0.025 emu/g and 60 Oe respectively is due to the Ag impurity on the surface of the Ag-Cu nanoparticle. The above analysis interestingly illustrates that for lower concentrations of Fe, the microstructure for Ag-Fe nanoparticles is characterized by the presence of an Ag-Fe solid solution shell and a pure Ag core phases instead of a pure Ag core and pure Fe or Fe-oxide shell configuration. A pure Ag-core and Fe/Fe-oxide-shell is expected due to a large immiscibility between Ag and Fe atoms in the bulk phase. A similar two phase microstructure containing a solid solution and a pure component phase for chemically synthesized Ag-Ni nanoparticles has been reported earlier by Srivastava et al. [2].

Conclusion

In conclusion, in the present work Ag-Fe nanoparticles were produced by the sonochemical route. As-synthesized nanoparticles revealed a compositionally graded microstructure along the particle radius. The regions at or near the surface of the particles were composed of both Ag and Fe atoms. The iron content gradually decreased towards the center of the particle. The core of the particle was made up of pure Ag. The magnetic characterization revealed the presence of a paramagnetic phase which indicated that the Ag and Fe atoms present in the particle were in a solid solution arrangement.

Acknowledgement

The authors acknowledge the electron microscopy facilities available at the Advanced Facility for Microscopy and Microanalysis (AFMM) at the Indian Institute of Science, Bangalore, India.

References

- [1] W. A. Jesser and C. T. Schamp, *Phys. Status Solidi (c)* 5, 539 (2008). <http://dx.doi.org/10.1002/pssc.200776825>
- [2] C. Srivastava, S. Chithra, K. D. Malviya, S. K. Sinha and K. Chattopadhyay, *Acta Materialia* 59, 6501 (2011). <http://dx.doi.org/10.1016/j.actamat.2011.07.022>
- [3] Robert E. Reed-Hill, *Physical Metallurgy Principles*, Litton Educational Publishing, New York, 1973.
- [4] Z. Peng and H. Yang, *J Solid State Chem.* 181, 1546 (2008). <http://dx.doi.org/10.1016/j.jssc.2008.03.013>
- [5] Z. Zhang, T. M. Nenoff, J. Y. Huang, D. T. Berry and P. P. Provencio, *J. Phys. Chem. C* 113, 1155 (2009). <http://dx.doi.org/10.1021/jp8098413>
- [6] C. Srivastava, *Mater. Lett.* 70, 122 (2012). <http://dx.doi.org/10.1016/j.matlet.2011.11.079>
- [7] B. N. Wanjala, J. Luo, B. Fang, D. Mott and C. J. Zhong, *J. Mater. Chem.* 21, 4012 (2011). <http://dx.doi.org/10.1039/c0jm02682d>
- [8] C. W. Hills, N. Mack and R. G. Nuzzo, *J. Phys. Chem. B* 107, 2626 (2003). <http://dx.doi.org/10.1021/jp022182k>
- [9] D. A. Porter and K. E. Easterling, *Phase Transformations in Metal and Alloys*, CRC Press, Taylor & Francis Group, Boca Raton, 2009.
- [10] C. Srivastava and B. M. Mundotiya, *Electrochem Solid St.* 15, K10 (2012). <http://dx.doi.org/10.1149/2.003202es1>
- [11] J. H. He, H. W. Sheng and E. Ma, *Appl. Phys. Lett.* 78, 1343 (2001). <http://dx.doi.org/10.1063/1.1352040>
- [12] J. H. Bang and K. S. Suslik, *Adv. Mater.* 22, 1039 (2010). <http://dx.doi.org/10.1002/adma.200904093>
- [13] L. J. Swartzendruber, *J. Phase Equilib.* 5, 560 (1984).
- [14] B. D. Cullity and C. D. Graham, *Introduction to Magnetic Materials*, John Wiley and Sons Inc, New Jersey, 2009.
- [15] K. Santhi, E. Thirumal, S. N. Karthick, H. J. Kim, M. Nidhin, V. Narayanan and V. Stephen, *J. Nanopart. Res.* 14, 868 (2012). <http://dx.doi.org/10.1007/s11051-012-0868-7>
- [16] Y. Jo, M. H. Jung, M. C. Kyum, K. H. Park and Y. N. Kim, *J. Magnetism* 11, 160 (2006).